

# Dynamics of Resistance Development to Imatinib under Increasing Selection Pressure: A Combination of Mathematical Models and In Vitro Data

Benjamin Werner<sup>1\*</sup>, David Lutz<sup>2</sup>, Tim H. Brümmendorf<sup>3</sup>, Arne Traulsen<sup>1</sup>, Stefan Balabanov<sup>2</sup>

**1** Evolutionary Theory Group, Max-Planck-Institute for Evolutionary Biology, Plön, Germany, **2** Department of Oncology, Hematology, Bone Marrow Transplantation and Pneumology, Hubertus Wald Tumor Zentrum, University Hospital Eppendorf, Hamburg, Germany, **3** Department Hematology and Oncology, RWTH Medical School, Aachen, Germany

## Abstract

In the last decade, cancer research has been a highly active and rapidly evolving scientific area. The ultimate goal of all efforts is a better understanding of the mechanisms that discriminate malignant from normal cell biology in order to allow the design of molecular targeted treatment strategies. In individual cases of malignant model diseases addicted to a specific, ideally single oncogene, e.g. Chronic myeloid leukemia (CML), specific tyrosine kinase inhibitors (TKI) have indeed been able to convert the disease from a ultimately life-threatening into a chronic disease with individual patients staying in remission even without treatment suggestive of operational cure. These developments have been raising hopes to transfer this concept to other cancer types. Unfortunately, cancer cells tend to develop both primary and secondary resistance to targeted drugs in a substantially higher frequency often leading to a failure of treatment clinically. Therefore, a detailed understanding of how cells can bypass targeted inhibition of signaling cascades crucial for malignant growths is necessary. Here, we have performed an in vitro experiment that investigates kinetics and mechanisms underlying resistance development in former drug sensitive cancer cells over time in vitro. We show that the dynamics observed in these experiments can be described by a simple mathematical model. By comparing these experimental data with the mathematical model, important parameters such as mutation rates, cellular fitness and the impact of individual drugs on these processes can be assessed. Excitingly, the experiment and the model suggest two fundamentally different ways of resistance evolution, i.e. acquisition of mutations and phenotype switching, each subject to different parameters. Most importantly, this complementary approach allows to assess the risk of resistance development in the different phases of treatment and thus helps to identify the critical periods where resistance development is most likely to occur.

**Citation:** Werner B, Lutz D, Brümmendorf TH, Traulsen A, Balabanov S (2011) Dynamics of Resistance Development to Imatinib under Increasing Selection Pressure: A Combination of Mathematical Models and In Vitro Data. PLoS ONE 6(12): e28955. doi:10.1371/journal.pone.0028955

**Editor:** Mikhail V. Blagosklonny, Roswell Park Cancer Institute, United States of America

**Received:** October 16, 2011; **Accepted:** November 17, 2011; **Published:** December 22, 2011

**Copyright:** © 2011 Werner et al. This is an open-access article distributed under the terms of the Creative Commons Attribution License, which permits unrestricted use, distribution, and reproduction in any medium, provided the original author and source are credited.

**Funding:** The authors have no support or funding to report.

**Competing Interests:** The authors have declared that no competing interests exist.

\* E-mail: werner@evolbio.mpg.de

## Introduction

The variety of approaches in cancer research ranges from clinical studies, experimental studies in vivo and vitro and genetic analysis to computational and mathematical models. Due to the insights from all these domains it was possible to develop specific targeted therapies for many cancer types and maybe cures for some are within reach [1]. A very promising example is the progress in treatment of patients with chronic myeloid leukemia (CML). CML is caused by a single reciprocal chromosomal translocation between the long arms of chromosome 9 and 22, the so called Philadelphia chromosome, in a hematopoietic stem cell [2]. The resulting BCR-ABL fusion gene encodes for a constitutive active tyrosine kinase, which is expressed and active in almost all haematopoietic cells and which leads to accelerated cell cycle activity [3]. As a result predominantly white blood cells at all stages of differentiation are significantly increased in peripheral blood and bone marrow of affected patients. Some years ago the standard treatment in the chronic phase was interferon-alpha and after disease progression chemotherapy with or without hemato-

poietic stem cell transplantation, a procedure that is associated with significant side effects and risks. The treatment algorithms changed due to the development of tyrosine kinase inhibitors (TKI) such as Imatinib [4], Nilotinib [5], Dasatinib [6] and Bosutinib [7]. These molecules bind specifically to the kinase domain of BCR-ABL and thereby strongly suppress the proliferation capability of CML cells. Since normal cells are less affected by this treatment, it allows normal hematopoiesis to be restored [8]. Long time clinical studies investigating the effect of TKIs show overwhelming success [4,9,10]. Unfortunately, there are cases in which patients do not respond to the drug or develop resistance during the treatment. This raises the question of how BCR-ABL positive cells bypass inhibition and develop resistance. A large number of in vivo and in vitro studies were performed, which identified different mutations causing resistance to TKIs [11,12]. However, the spatial structure and thus the molecular mechanism of kinase domain binding varies between different tyrosine kinase inhibitors and thus clones resistant to one inhibitor may be sensitive to an alternative inhibitor. Unfortunately, there are clones resistant to several inhibitors at the same time. For example

the mutation T315I, the so called gatekeeper mutation, causes resistance to all approved TKIs. Agents as Ponatinib have been particularly designed to bind to such mutated kinase domains of BCR-ABL and suppress cell proliferation. These are in clinical trials and showing promising results [13–15]. Also many mathematical models concentrate on the probabilities and the dynamics of the development of such cross resistance and how to reduce the risk of resistance evolving to a minimum using combination therapies of different drugs [16–18]. We will not focus on this aspect in the following, but address the dynamics of resistance development instead.

Here, we discuss an experimental setup that induces resistance to Imatinib in initially sensitive BCR-ABL positive Ba/F3-p210 cells. In the following our aim is not to assess the probability of the occurrence of a specific resistance-conferring mutations nor to identify novel mutations, but to focus on the clonal dynamics that occurs during such an experimental setup. Instead, we show that not only mutations, but also intracellular processes that do not lead to any mutations can lead to the development of resistance. We investigate the average fitness of cancer cells exposed to a drug concentration that increases over time in this *in vitro* experiment. Basic features of this dynamic can be explained by a mathematical model, assuming a fitness of cancer cells that decreases with time as the drug concentration increases. By comparing the experimental data with simulation and analytical results we were able to assess individual parameters in this model and gain insights into the general cancer cell population dynamics under such environmental situations.

## Materials and Methods

### Materials

Imatinib was purchased from Toronto Research Chemicals Inc, Ontario, Canada. Stock solutions of IM (10 mg/mL; in DMSO/H<sub>2</sub>O (1:1)) was stored at 20°C. Murine BCR-ABL transduced pro-B cell line Ba/F3-p210 was obtained from N.P. Shah and C.L. Sawyers (UCLA, USA). Cells were cultured under standard conditions as previously described [19].

### Cell culture approach for induction of Imatinib resistance

In this experiment, Ba/F3-p210 cells carrying the BCR-ABL kinase were used as a model for resistance development to IM treatment, following a well established protocol [20]. Flow cytometry based cell sorting using a FACSAria (BD Biosciences) was employed to produce 10 clones of BaF/3-p210 cells. These clones were expanded to cultures of  $2 \times 10^5$  cells each. These cultures were exposed to Imatinib in a concentration increasing over time, starting with 0.1  $\mu$ M. Cell viability was measured by the Trypan blue exclusion method [21]. The Imatinib concentration was periodically increased by 0.1  $\mu$ M only if cell viability was above 70%, the concentration stays unchanged if the cell viability is between 30% and 70% and withdrawn in case of cell viability less than 30%. Thus the time the Imatinib concentration was increased differed for different clone lines, but the concentration was always increased within 12 days. Parallel, a control with untreated clones was performed. At the end of the experiment all Imatinib treated lineages were resistant to the drug, confirmed by a cytotoxicity MTT-assay.

### MTT assay

The 3-(4,5-dimethylthiazol-2-yl)-2,5-diphenyltetrazoliumbromide (MTT) assay was performed as previously described [22]. In brief, BAF/3-p210 cells were plated into 96-well flat-bottomed microtiter plates (Becton Dickinson, Heidelberg, Germany) at

$1.5 \times 10^4$  cells/well in 150  $\mu$ M of their respective media. Cells were preincubated for 24 hours before increasing concentrations of Imatinib (0–10  $\mu$ M) were added. All analyses were performed in triplicates. After 48 hours, the viable cells in each well were assayed. The dose-response effect for Imatinib at the point of inhibitory concentration (IC<sub>50</sub>) was analyzed by the median-effect method with CalcuSyn Software (Biosoft, Cambridge, United Kingdom) [23].

### Mutagenesis screen and real time PCR for BCR-ABL transcript

To identify possible BCR-ABL kinase domain mutations as mechanism of Imatinib resistance, the coding cDNA of the kinase domain was sequenced. For all RT-PCR reactions, total RNA was isolated using TRIzol (Invitrogen). cDNA was prepared by reverse transcription of 250 ng RNA with oligo(dT)15 and Superscript II reverse transcriptase (Invitrogen) and amplified using REDTaq ReadyMix PCR Reaction Mix (Sigma-Aldrich). BCR-ABL allele was amplified by nested PCR using BCR forward primer B2A(5'-TTCAGAAGCTTCTCCCTGACAT-3') and ABL reverse primer 4065 (5'-CCTTCTCTAGCAGCTCATAACACCTG-3'). Nested PCR reactions were performed using BCR F4 forward (5'-ACAGCATTCCGCTGACCATCAATA-3') and reverse U396 (5'-GCCATAGGTAGCAATTTCCC). PCR products containing the kinase domain were sequenced with both forward primer 3306F (5'-TGGTTCATCATCATTCAACGG-3') and reverse primer 4000R (5'-GGACATGCCATAGGTAGCA-3'). Real time PCR for BCR-ABL was performed as previously described [24,25]. Amplification of ABL was used as a internal housekeeping gene.

### Quantification of MDR-1 on resistant clones

For the relative quantification of MDR-1 we used a flow cytometry-based assay. Cells were fixed in 2% formaldehyde for 10 minutes at 37°C, chilled on ice for 1 minute, and then permeabilized with ice-cold 90% methanol for 30 minutes on ice. From each sample,  $2 \times 10^5$  cells were washed with 2 mL incubation buffer (PBS/0.5% bovine serum albumin), centrifuged at 50 g for 5 minutes, and resuspended in 100  $\mu$ L of incubation buffer with 2.0  $\mu$ L of a MDR-1 specific antibody (abcam, Cambridge, UK). After 45 minutes of incubation at RT, cells were washed twice, resuspended in 100  $\mu$ L incubation buffer with 0.5  $\mu$ L of the secondary antibody (anti-rabbit IgG FITC-conjugate; Jackson ImmunoResearch Europe, Newmarket, United Kingdom), and incubated at RT for 30 minutes in the dark. After washing two times with washing buffer cells were analysed using flow cytometry.

### Individual based model

We compare the dynamics in the mathematical model to the experiment based on the fitness of cells. We assume that the average fitness of the experimental cell population is the ratio between the number of vital cells and the total number of cells. Mathematically we model the cell population dynamics observed in the experiment by an individual based stochastic approach, applying a standard two type Moran process [26,27]. We assume a population of  $N = 2 \times 10^5$  cells consisting of two subpopulations, wild type leukemic cancer cells sensitive to Imatinib and Imatinib resistant cancer cells. Initially, only wild type cancer cells are present, but transformations from wild types into the resistant type are possible. In each time step, one cell is chosen to reproduce and one cell is chosen to die, thus the total number of cells stays constant and the subpopulation sizes can change at most by 1 cell

during one time step, see Fig. 1. If a wild type cancer cell is chosen to reproduce, an Imatinib resistant cancer cell is produced with a transformation probability  $u$ . To avoid complications, we assume that resistant types cannot switch back to nonresistant types. This would not change the basic results, however. The two types differ in their fitness  $f_w$  (for the wild type) and  $f_r$  (for the resistant type). We assume a time dependent wild type fitness function, due to the increasing concentration of Imatinib in the experiment. We set the fitness of untreated wild types  $f_w$  to one and assume that it decreases linearly with increasing Imatinib concentration,

$$f_w(t) = \begin{cases} 1 - \frac{t}{t^*} & 0 \leq t \leq t^* \\ 0 & \text{otherwise.} \end{cases} \quad (1)$$

The parameter  $t^*$  determines the impact of Imatinib on wild type cells. Choosing other decreasing functions, e.g. an exponentially decreasing function, does not change the results qualitatively. For the Imatinib resistant subpopulation we assume constant fitness,  $f_r = \text{const}$ . For  $f_r < f_w$ , resistant cells proliferate slower than wild type cells, for  $f_r > f_w$  they proliferate faster than wild type cells. The experimental data suggest  $0 < f_r < 1$  and thus initially resistant types would initially be out-competed by wild type cells, see below. Due to the decreasing fitness of wild type cells, we can go from one domain to the other in time. We assume that cell

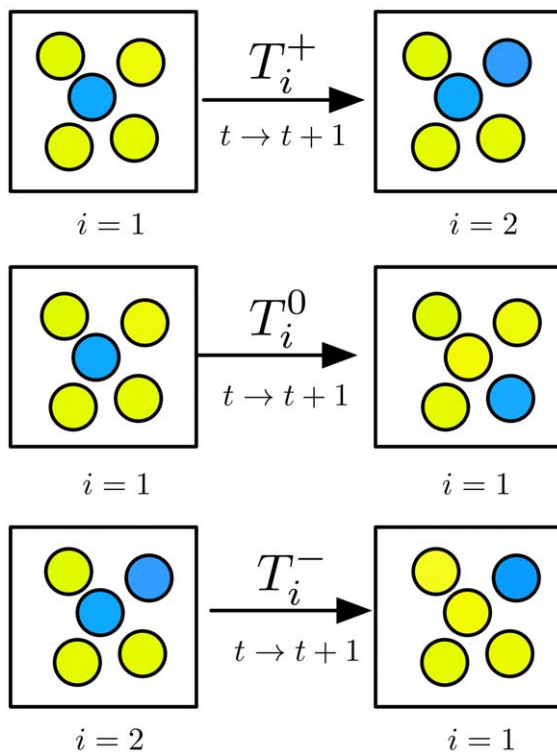


**Figure 1. Individual based stochastic simulation as two type Moran process.** We assume two possible cell types, wild type leukemic cancer cells sensitive to Imatinib (yellow) and resistant cancer cells (blue). In total,  $\approx 2 \times 10^5$  cells were included in the experiment and simulations. At time  $t$  there are  $i$  resistant cells and  $N-i$  wild type cells. During the next time step  $t+1$  three cases are possible: (i) the number of resistant cells increases by one with probability  $T_i^+$ , (ii) stays the same with probability  $T_i^0 = 1 - T_i^+ - T_i^-$  (iii) or decreases by one with probability  $T_i^-$ , (see equation (2a) and (2b)). doi:10.1371/journal.pone.0028955.g001

reproduction occurs proportional to fitness and simultaneously a random cell is chosen to die. Thus, the probability of increasing or decreasing the number of resistant cancer cells  $i$  at time  $t$  is notated by  $T_i^+$  or  $T_i^-$  respectively,

$$T_i^+ = \left[ \frac{if_r}{if_r + (N-i)f_w} + u \frac{(N-i)f_w}{if_r + (N-i)f_w} \right] \frac{N-i}{N} \quad (2a)$$

$$T_i^- = \left[ (1-u) \frac{(N-i)f_w}{if_r + (N-i)f_w} \right] \frac{i}{N}. \quad (2b)$$

The number of resistant cells stays unchanged with probability  $T_i^0 = 1 - T_i^+ - T_i^-$ . One generation consists of  $N$  reproduction and death events, such that each cell reproduced on average once.

### Analytical approximation for large population size

If the population size  $N$  is large, we can describe the averages of our individual based model by a deterministic approach. In this case, we consider the frequency (relative population size) of the two cell types, wild type leukemic cells with frequency  $w(t) = (N-i)/N$  and Imatinib resistant cell types with frequency  $r(t) = i/N$ . We use the same fitness functions as above and also assume transformations from the wild type to the resistant type. The average fitness of the system, which has been measured in the experiment, is given by  $\Phi(t) = w(t)f_w(t) + r(t)f_r$ . The change in wild type and resistant type frequencies for large populations are given by a replicator mutator equation [27,28]

$$\dot{w} = w(f_w - \Phi) - uf_w w \quad (3a)$$

$$\dot{r} = r(f_r - \Phi) + uf_w w, \quad (3b)$$

where the dot represents a derivative with respect to time  $t$ . With the functions from above, these differential equations take the form

$$\dot{w} = \begin{cases} w(1-w) \left( 1 - f_r - \frac{t}{t^*} \right) - u \left( 1 - \frac{t}{t^*} \right) w & 0 \leq t \leq t^* \\ w(1-w) (-f_r) & t > t^* \end{cases} \quad (4a)$$

$$\dot{r} = \begin{cases} r(1-r) \left( f_r - 1 + \frac{t}{t^*} \right) + u \left( 1 - \frac{t}{t^*} \right) w & 0 \leq t \leq t^* \\ r(1-r) f_r & t > t^*. \end{cases} \quad (4b)$$

These are time dependent nonlinear differential equations of the Bernoulli type, for which a general solution scheme exist [29]. Thus the system of differential equations can be reduced to integrals, which in this situation are solvable. Due to  $w(t) + r(t) = 1$ , we only have to solve one of the equations. The general solution for  $w(t)$  with respect to the initial condition  $w(0) = 1$  for  $t \leq t^*$  reads

$$w(t) = \frac{1-u}{1 - u e^{h_t^2 - h_0^2} + \sqrt{\frac{\pi t^*}{2}} \frac{u f_r}{\sqrt{1-u}} e^{h_t^2} [\text{Erf}(h_t) - \text{Erf}(h_0)]}, \quad (5)$$

where 
$$h_t = \frac{(1-u) \frac{t}{\sqrt{t^*}} + \sqrt{t^*} (f_r - 1 + u)}{\sqrt{2(1-u)}} \quad \text{and}$$

$\text{Erf}(h_t) = \frac{2}{\sqrt{\pi}} \int_0^{h_t} ds e^{-s^2}$  is the error function. For  $t \ll 1$ , this can be approximated by

$$w(t) \approx 1 - ut + u \frac{1 + (1 + u - f_r)t^*}{2t^*} t^2 + o[t^3].$$

For  $t \geq t^*$ , the number of resistant cells grows logistically and consequently, the number of wild type cells decreases logistically

$$w(t) = \frac{1}{1 + \frac{1 - w(t^*)}{w(t^*)} e^{-f_r(t-t^*)}}. \quad (6)$$

The average fitness of the total population becomes

$$\Phi(t) = f_r(1 - w(t)) + \left(1 - \frac{t}{t^*}\right)w(t). \quad (7)$$

For small  $t$ , when  $w(t)$  is approximately constant, the average fitness decreases approximately linearly determined by  $t^*$ .

## Results

### Development of Imatinib resistance in cell culture

Using an in vitro approach to induce Imatinib resistance under increasing selection pressure, we detected resistance in 10 out of 10 BAF/3-p210 clones. As depicted in Fig. 2A the development of Imatinib resistance was associated with a significant decrease in the population doubling compared to control cells. The observed development of Imatinib resistance resulted in an significant increase of the  $\text{IC}_{50}$  for Imatinib in all, but one clones (Fig. 2 B). For four resistant clones, it was possible to identify previously known resistance mutations in the BCR-ABL kinase domain. These were the D276G (prevents Imatinib from binding to BCR/ABL), E355G (blocks the TK catalytic centre) and L284M (inactivates the kinase) mutations (Fig. 2 C). No mutations of the kinase domain were found in the other clones, nevertheless they also developed resistance to Imatinib. In order to explore if the resistance in the non-mutated clones is based on an increased BCR-ABL expression we employed real time PCR for quantification of the BCR-ABL transcript. As depicted in Fig. 2 D we could only identify an up-regulation of BCR-ABL expression in one single clone. Furthermore, there was no increased expression of the ABC-transporter MDR-1 on resistance cell clones (Fig. 2 E). Based on these findings, we concluded that mechanisms other than kinase domain mutations, BCR-ABL over expression or MDR-1 up-regulation have lead to resistance in these cases.

### Fitting the mathematical model to the experimental data

We now focus on the dynamics of the cell population. Initially, the average fitness of the total population decreases as the Imatinib concentration increased. At day 24 of the experiment, a global fitness minimum of  $\Phi = 0.706$  (experimental data) is obtained (Fig. 3 A). Subsequently, the average population fitness increased, although the environmental conditions become more challenging due to the ongoing increase of the Imatinib concentration. From day 48 until the end of the experiment the average fitness of the population was saturated and fluctuated around  $\Phi = 0.83 \pm 0.03$ . Our mathematical model offers a simple explanation for this result: In the

beginning, only wild type cancer cells with decreasing fitness are present (Fig. 3 B). During the experiment, the frequency of resistant cell types increased and once they represent the bulk of the population, the average population fitness becomes independent of a further increase of Imatinib concentration. Consequently, the average fitness becomes constant. While it is challenging to analyze the underlying mechanisms of resistance evolution, we were able to address the parameter ranges in the experiment based on our model.

First, we fixed time scales to make experimental and simulation results comparable. In the control experiment, untreated wild type cancer cells were grown in a regular growth medium and the population doubling times were recorded. We compare these doubling times to one generation in our simulation, which we define here as  $N$  reproduction events in a population of size  $N$ . We found on average a doubling rate of  $0.48 \pm 0.01$  per day in the experiment, thus one generation in silico approximately relates to two days in vitro.

The initial fitness decrease was determined by the fitness decrease of wild type cells only and thus allowed us to fix the parameter  $t^*$  by linear regression of the average population fitness on day 0, 12 and 24, leading to  $t^* = 82 \pm 4$  days. Thus, assuming a linear decrease of fitness according to equation (1) the wild type fitness would reach zero on day 82 of the experiment (dashed black line in Fig. 3 A). Such an assumption of zero fitness is probably biologically not meaningful. However, our simulation results remain unchanged if we assume that the lowest possible fitness value of wild type cells is 0.5. This would be reached at day 40 of the experiment, where the resistant cell type already took over the population as shown in Fig. 3 B.

In our model the average fitness of the total population becomes constant at high Imatinib concentrations, because the resistant cell types take over the cell cultures. This fixed the average fitness of the resistant cell types to  $f_r = 0.83 \pm 0.02$  (averaged from day 48 on).

The only remaining free parameter is the switching probability  $u$ , which is more difficult to assess. To determine  $u$ , we fixed  $t^*$  and  $f_r$  as discussed above and performed individual based stochastic simulations, which suggests that a switching probability between  $10^{-6} \leq u \leq 10^{-4}$  is compatible with the experiment. Smaller values of  $u$  would cause a later increase in frequency of resistant cell types, but as soon as a certain fraction of resistant cells are present they fixate faster. For higher values of  $u$  the minimum of the average fitness  $\Phi$  would be reached earlier. We also performed a non linear fit of equation (7) with the full solution for  $w(t)$ , equation (5). The best fit yields a value of  $u = 10^{-4}$ . Note that  $u = 10^{-4}$  is too high to call this parameter a mutation rate. However, in the experiment only in 4 out of 10 samples mutations known for causing resistance to Imatinib were found.

To take these two different experimental outcomes into account, we performed the procedure described above independently for samples with and without mutations. The result is shown in Fig. 4. In samples where mutations were detected, we observe  $u = 1 \times 10^{-6}$ ,  $f_r = 0.88$ . In the case of no detected mutations, we found  $u = 6 \times 10^{-4}$  and  $f_r = 0.82$ . Thus, the transformation probability differs by magnitudes and samples with mutations seemed finally fitter than samples without mutations. This leads to the possibility that two mechanism may cause resistance, mutation and a sort of phenotype switching. We extended our model to incooperate these two distinct effects, as shown in Fig. 5. With this extension, wild type cells switch into mutated cells (M) with probability  $u_M = 1 \times 10^{-6}$  and fitness  $f_M = 0.88$ . Alternatively, they switch into transformed types (T) with probability  $u_T = 6 \times 10^{-4}$  and fitness  $f_T = 0.82$ . Additionally, transformed types (T) can mutate with probability  $u_M$  into mutated types (M).

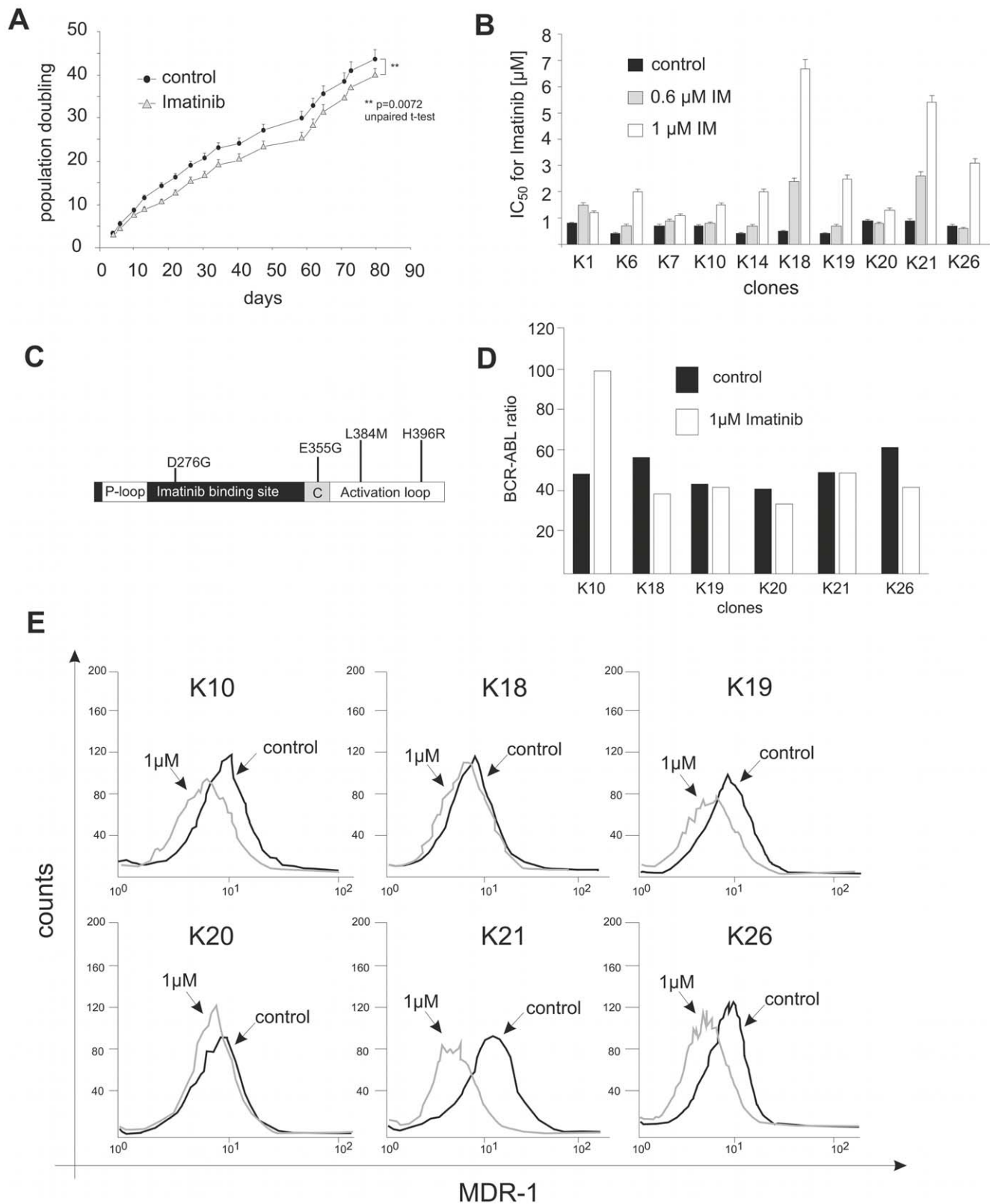


**Figure 2. Experimental results.** **A**) Average population doubling time observed for BAF/3-210 cells with (white triangles) and without (black dots) long-term Imatinib treatment. The number of population doubling for control cells was significantly higher compared to IM-treated cells. **B**) Measurement of  $IC_{50}$  for Imatinib in control and resistant clones. The long-term presence of Imatinib increase the  $IC_{50}$  in all resistant cell clones. In particular, cell clones which were growing at 1 M Imatinib showed a marked increase of the  $IC_{50}$  value. The cell viability was determined using MTT assay and  $IC_{50}$  was calculated CalcuSyn software. **C**) Schematic representation of in vitro detected BCR-ABL mutations. **D**) Quantification of BCR-ABL transcript by real-time PCR in resistant clones without BCR-ABL mutations. Only one clone (K10) exhibited an increased expression of BCR-ABL. **E**)

Quantification of MDR-1 expression by flow cytometry in resistant clones without BCR-ABL mutations. Imatinib resistance was not associated with an increased expression of MDR-1.

doi:10.1371/journal.pone.0028955.g002

The dynamics for this scenario is shown in Fig. 5 C. Initially only wild type cells are present in the simulation. Due to the higher switching probability transformed types take over almost the whole population, but due to their fitness advantage and the directed mutations in the long run the mutant types fixate. However the experiment was stopped after 120 days. In the experiment we found mutant types in 4 out of 10 samples. At this time we observe frequencies of 0.43 for mutated types and 0.57 for transformed types in the simulation, compatible with the experiment. Also in the simulation, the average fitness of the population goes through a minimum, but the fitness still increases after 120 days, because the mutant type does not reach fixation yet.

## Discussion

Resistance to TKI is a frequent clinical problem in treatment of CML patients. The appearance of resistant cell clones undermines our ability to control the malignant BCR-ABL positive cell clone and thereby prevent the successful treatment of CML patients. The mechanisms of TKI resistance are either BCR-ABL dependent or BCR-ABL independent [30]. Mutations in the BCR-ABL kinase domain represent the most frequent BCR-ABL dependent mechanisms. On the other hand, overexpression of BCR-ABL and overexpression of drug transporters are known kinase independent mechanisms of TKI resistance. The rise of

drug resistance is a evolutionary process characterized by a competition between sensitive and resistant cells but not an active process of resistance induction by the drug [31].

Using a combination of a clonal in vitro approach for induction of Imatinib resistance and mathematical modeling, we were able to explain the dynamics of the average fitness of Imatinib treated cancer cell populations in vitro in a simple model assuming that:

- The population consists of only three subpopulation, the wild type cancer cells (the only cell type present at the beginning of the experiment) and resistant cell types (mutated and transformed cells).
- The fitness of wild type cells decreases with increasing drug concentration over time. The fitness of resistant types is lower than the wild type fitness, but both are constant.
- We introduced directed transformation. Wild types transform into resistant types, the reversal is neglected.

With these assumptions, we provided a method to fix the model parameters and thus get some insights into the mechanism that cause the dynamics. Comparing the analytical solution with experimental results enabled us to fix important parameter of the system. Accordingly, it is possible to derive a range for the transformation probability  $u$ , which is  $10^{-6} \leq u \leq 10^{-4}$  for this experimental setup. This is high compared to values normally assumed for mutations, which seems to be about  $10^{-8}$  for normal cells. But the mutation rate of malignant cells has been reported to be at least  $10^{-1}$  to  $10^{-2}$  higher [32,33]. If we perform our analysis separately for the samples with and without mutations, we find different parameter values. For the mutated cell lines, we found  $u_M = 1 \times 10^{-6}$ , which is in the expected range for mutation rates of such malignant cells. But for samples without mutations, we find  $u_T = 6 \times 10^{-4}$ . This supports the idea that not only mutations are responsible for drug resistance evolution in this case, but that also other mechanisms are likely to be involved [34]. Noteworthy, we could not detect BCR-ABL- or MDR-1 overexpression as the reason for resistance. However, there is some evidence that an activation of additional pathways, like the phosphatidylinositol-3-kinase (PI3K)-AKT pathway [20] or Src family kinase [35,36], can compensate for the BCR-ABL inhibition and can promote the proliferation of these cells in the presence of Imatinib. From our mathematical model and our experimental results, one can conclude that particularly the time frame between day 24 and day 48 is crucial for development of resistance. It can be speculated that starting with day 24, the cells launch out to adapt their metabolism to the increasing pressure of raising Imatinib concentrations. This kind of adaptations are normally accompanied by an activation of novel signaling pathways and can drive the cellular metabolism of resistant cells to an increased glycolytic activity and phospholipid turnover [37,38]. In this context, our model represents a basis to determine the critical time point and Imatinib concentration for further studies to detect novel BCR-ABL independent resistance mechanisms. This should be done by a comprehensive and integrative genome-, transcriptome-, proteome- and metabolome analysis and may lead to additional insights into activated pathways of resistant CML cells. Recent in vitro and in silico studies have revealed that a combination of drugs with different mode of actions can prevent treatment failures due to drug resistance [16–18,39]. However, the appropriate targets are not defined and must be elucidate in further studies.

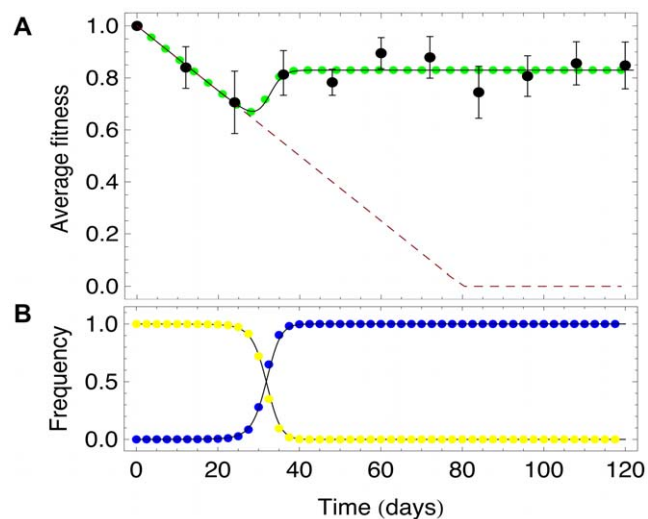


**Figure 3. Dynamics of resistance development in the experiment and the mathematical model.** **A)** Average fitness of the total population due to experiments (black dots), stochastic simulations (green dots) and analytical results (black line, due to equation (7)). The parameters of simulation and calculation were chosen to  $N = 2 \times 10^5$ ,  $u = 1 \times 10^{-4}$ ,  $t^* = 80$  days and  $b = 0.83$ . The dashed red line shows the linear decrease of the wild type fitness, the slope is determined by the critical time  $t^*$ . **B)** The average frequency of wild type cells due to simulation (yellow dots) and calculation (black line), as well as the frequency of resistant cancer cells (blue dots) over time. We always start with wild types only, but since the system selects for resistant cells, they fixate in the long run. This is why the average fitness of the total population exhibits a minimum. At the start of the experiments, the fitness of wild types decreases, but after some time resistant cells take over and the fitness increases until it saturates.

doi:10.1371/journal.pone.0028955.g003

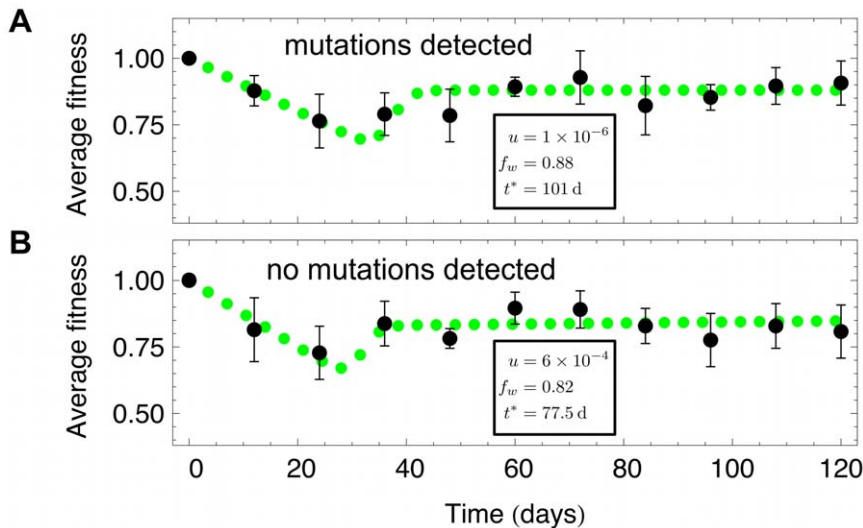


**Figure 4. Average fitness observed for samples A) with and B) without detected mutations.** The black dots are due to data and the green dots due to simulations. The evaluated parameters differ (see the inset of the plots), the fitness of the mutated cells is on average higher but their transformation rate is much smaller.

doi:10.1371/journal.pone.0028955.g004

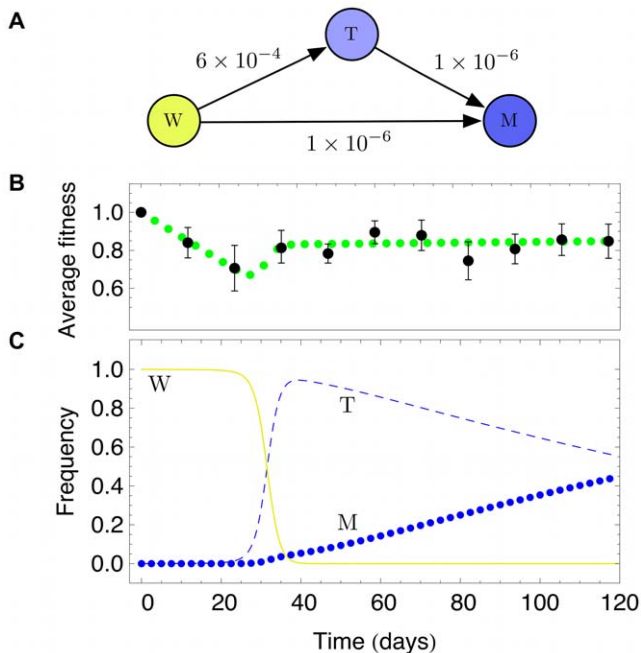


**Figure 5. Stochastic simulations with three subpopulations.** A) Transitions between the three types considered, wild types (W), resistant types without observed mutations (T) and resistant types with observed mutations (M). The switching probabilities are according to the arrows. B) Average fitness of the system described in a) due to simulations (green dots) and experimental data (black dots, as described in figure 3). The parameters are those observed in figure 4. C) Average frequency of the three types. Initially, only wild types (yellow line) are present, at day 37 of the experiment resistant types without observed mutations (T, dashed blue line) reach almost fixation, but in the long run mutated types (M, blue dots) take over due to their fitness advantage. At day 120 of the experiment we have 0.57 T types and 0.43 M types (6 T and 4 M types were observed in the experiment at day 120).

doi:10.1371/journal.pone.0028955.g005

From our study, it is apparent that the development of Imatinib resistance is associated with reduced fitness of resistant cells in vitro. Translating this into fitness in vivo can be challenging, due to additional aspects as the hierarchical structure of hematopoiesis [40–42], failed targeting of cancer stem cells, for example due to quiescent cells, [43,44] and possible aging effects [45]. Furthermore very small differences in vitro can cause important measurable differences in vivo, but also in this case mathematical approaches can be helpful [46]. Notably, the fitness of clones harboring a BCR-ABL mutation was higher compared to the unmutated clones. This might be due to the proposed switch on alternative or additional programs in unmutated clones which may be costly in terms of proliferation, but enable the cell to function independent of the BCR-ABL kinase. Based on recent studies, it can be speculated that in mutated clones the mutations are preexisting and the cells do not need to adapt their metabolism to reach resistance [47]. In this case the reduced fitness reflect the differences between mutant and wild-type BCR-ABL. Recent studies have revealed that certain mutated BCR-ABL kinases are accompanied by reduced oncogenic activity [48,49]. These findings are supported by clinical studies. Hanfstein et al. have shown a deselection of mutant BCR-ABL positive clones after cessation of tyrosine kinase inhibitor [50], as also suggested by mathematical models [8,51]. Fitness costs are commonly associated with drug resistance. Particularly, resistance against antibiotics is frequently observed in vitro and in vivo and is associated with reduced fitness of resistant clones [52,53]. In comparison to that, the existence of a fitness cost in resistance to cancer drugs has not been analysed in detail yet. Therefore, our data represent an appropriate model to further investigate in this cellular behavioral pattern.

## Acknowledgments

We thank Silke Zeschke for her technical assistance in this work. Further we thank David Dingli and Tom Lenaerts for helpful discussions on this manuscript.

## Author Contributions

Conceived and designed the experiments: SB THB. Performed the experiments: DL SB. Analyzed the data: BW DL AT SB. Wrote the paper: BW THB AT SB. Conceived and designed the mathematical model: BW AT.

## References

- Mahon FX, Ra D, Guilhot J, Guilhot F, Huguet F, et al. (2010) Discontinuation of imatinib in patients with chronic myeloid leukaemia who have maintained complete molecular remission for at least 2 years: the prospective, multicentre stop imatinib (stim) trial. *Lancet Oncol*. pp 1029–1035.
- Rowley JD (1973) Letter: A new consistent chromosomal abnormality in chronic myelogenous leukaemia identified by quinacrine uorescence and giemsa staining. *Nature* 243: 290–293.
- Deininger M, Goldman JM, Melo JV (2000) The molecular biology of chronic myeloid leukemia. *Blood* 96: 3343–3356.
- Druker BJ, Guilhot F, O'Brien SG, Gathmann I, Kantarjian H, et al. (2006) Five-year follow-up of patients receiving imatinib for chronic myeloid leukemia. *The New England Journal of Medicine* 355: 2408–2417.
- Weisberg E, Manley PW, Breitenstein W, Brügger J, Cowan-Jacob SW, et al. (2005) Characterization of amn107, a selective inhibitor of native and mutant bcr-abl. *Cancer Cell* 7: 129–141.
- Shah NP, Tran C, Lee FY, Chen P, Norris D, et al. (2004) Overriding imatinib resistance with a novel abl kinase inhibitor. *Science* 305: 399–401.
- Cortes J, Kantarjian H, Brümmendorf T, Kim D, Turkina A, et al. (2011) Safety and efficacy of bosutinib (ski-606) in chronic phase philadelphia chromosome-positive cml patients with resistance or intolerance to imatinib. *Blood* 355594.
- Lenaerts T, Pacheco JM, Traulsen A, Dingli D (2010) Tyrosine kinase inhibitor therapy can cure chronic myeloid leukemia without hitting leukemic stem cells. *Haematologica* 95: 900–907.
- Saglio G, Kim DW, Issaragrisil S, le Coutre P, Etienne G, et al. (2010) Nilotinib versus imatinib for newly diagnosed chronic myeloid leukemia. *N Engl J Med* 362: 2251–2259.
- Kantarjian H, Shah NP, Hochhaus A, Cortes J, Shah S, et al. (2010) Dasatinib versus imatinib in newly diagnosed chronic-phase chronic myeloid leukemia. *New Engl J Med* 326: 2260–2270.
- O'Hare T, Eide CA, Deininger MW (2007) Bcr-abl kinase domain mutations, drug resistance, and the road to a cure for chronic myeloid leukemia. *Blood* 110: 2242–2249.
- Bixby D, Talpaz M (2009) Mechanisms of resistance to tyrosine kinase inhibitors in chronic myeloid leukemia and recent therapeutic strategies to overcome resistance. *Hematology American Society of Hematology Education Program Book*. pp 461–476.
- Hochhaus A, La Rosée P, Müller MC, Ernst T, Cross NC (2011) Impact of bcr-abl mutations on patients with chronic myeloid leukemia. *Cell Cycle* 10: 250–260.
- Demidenko ZN, An WG, Lee JT, Romanova LY, McCubrey JA, et al. (2005) Kinase-addition and bi-phasic sensitivity-resistance of bcr-abl- and raf-1-expressing cells to imatinib and geldanamycin. *Cancer Biol Ther* 4: 484–490.
- O'Hare T, Shakespeare WC, Zhu X, Eide CA, Rivera VM, et al. (2009) Ap24534, a pan-bcr-abl inhibitor for chronic myeloid leukemia, potently inhibits the t315i mutant and overcomes mutationbased resistance. *Cancer Cell* 16: 401–412.
- Katouli AA, Komarova NL (2010) Optimizing combination therapies with existing and future cml drugs. *PLoS One* 5.
- Komarova NL, Wodarz D (2009) Combination therapies against chronic myeloid leukemia: short-term versus long-term strategies. *Cancer Res* 69: 4904–4910.
- Komarova NL, Katouli AA, Wodarz D (2009) Combination of two but not three current targeted drugs can improve therapy of chronic myeloid leukemia. *PLoS One* 4: e4423.
- Balabanov S, Gontarewicz A, Keller G, Radrizzani L, Braig M, et al. (2011) Abcg2 overexpression represents a novel mechanism for acquired resistance to the multi-kinase inhibitor danusertib in bcr-abl-positive cells in vitro. *PLoS ONE* 6: e19164.
- Burchert A, Wang Y, Cai D, Bubnoff N, Paschka P, et al. (2005) Compensatory pi3- kinase/akt/mtor activation regulates imatinib resistance development. *Leukemia* 19: 1774–1782.
- Patterson MK (1979) Measurement of growth and viability of cells in culture. *Methods Enzymol* 58.
- Balabanov S, Gontarewicz A, Ziegler P, Hartmann U, Kammer W, et al. (2007) Hypusination of eukaryotic initiation factor 5a (eif5a): a novel therapeutic target in bcr-abl-positive leukemias identified by a proteomics approach. *Blood* 109: 1701–1711.
- Chou TC, Talalay P (1981) Generalized equations for the analysis of inhibitions of michaelis-menten and higher-order kinetic systems with two or more mutually exclusive and nonexclusive inhibitors. *Eur J Biochem* 115: 207–216.
- Beillard E, Pallisaard N, van der Velden VHJ, Bi W, Dec R, et al. (2003) Evaluation of candidate control genes for diagnosis and residual disease detection in leukemic patients using 'real-time' quantitative reverse-transcriptase polymerase chain reaction (rq-pcr) - a europe against cancer program. *Leukemia* 17: 2474–2486.
- Gabert J, Beillard E, van der Velden VH, Bi W, Grimwade D, et al. (2003) Standardization and quality control studies of 'real-time' quantitative reverse transcriptase polymerase chain reaction of fusion gene transcripts for residual disease detection in leukemia - a europe against cancer program. *Leukemia* 17: 2318–2357.
- Moran PAP (1962) *The Statistical Processes of Evolutionary Theory*. Clarendon Press, Oxford, UK.
- Nowak MA (2006) *Evolutionary Dynamics*. Harvard University Press, Cambridge, MA.
- Page KM, Nowak MA (2002) Unifying evolutionary dynamics. *J Theor Biol* 219: 93–98.
- Bernoulli J (1695) Explicationes, annotationes, additiones ad ea, quae in actis sup. anni de curva elastica, isochrona paracentrica, velaria, hinc inde memorata, paratim controversa legundur; ubi de linea mediarum directionum, allisque novis. *Acta Eruditorum* 1: 65–80.
- von Bubnoff N, Peschel C, Duyster J (2003) Resistance of philadelphia-chromosome positive leukemia towards the kinase inhibitor imatinib (sti571, glivec): a targeted oncoprotein strikes back. *Leukemia* 17: 829–838.
- Blagosklonny MV (2002) Sti-571 must select for drug-resistant cells but 'no cell breathes fire out of its nostrils like a dragon'. *Leukemia* 16: 570–572.
- Drake JW, Charlesworth B, Charlesworth D, Crow JF (1998) Rates of spontaneous mutation. *Genetics* 148: 1667–1686.
- Hicks WM, Kim M, Haber JE (2010) Increased mutagenesis and unique mutation signature associated with mitotic gene conversion. *Science* 329: 82–85.
- Lange T, Park B, Willis SG, Deininger MW (2005) Bcr-abl kinase domain mutations in chronic myeloid leukemia: not quite enough to cause resistance to imatinib therapy? *Cell Cycle* 4: 1761–1766.
- Pene-Dumitrescu T, Smithgall TE (2010) Expression of a src family kinase in chronic myelogenous leukemia cells induces resistance to imatinib in a kinase-dependent manner. *J Biol Chem* 285: 21446–21457.
- Wu J, Meng F, Kong LY, Peng Z, Ying Y, et al. (2008) Association between imatinib-resistant bcr-abl mutation-negative leukemia and persistent activation of lyn kinase. *J Natl Cancer Inst* 100: 926–939.
- Klawitter J, Kominsky DJ, Brown JL, Klawitter J, Christians U, et al. (2009) Metabolic characteristics of imatinib resistance in chronic myeloid leukaemia cells. *Br J Pharmacol* 158: 588–600.
- Kominsky DJ, Klawitter J, Brown JL, Boros LG, Melo JV, et al. (2009) Abnormalities in glucose uptake and metabolism in imatinib-resistant human bcr-abl-positive cells. *Clin Cancer Res* 15: 3442–3450.
- Komarova NL (2011) Mathematical modeling of cyclic treatments of chronic myeloid leukemia. *Nath Biosci Eng* 8: 289–306.
- Dingli D, Pacheco JM (2006) Allometric scaling of the active hematopoietic stem cell pool across mammals. *PLoS One* 1: e2.
- Rodríguez-Brenes A, Komarova N, Wodarz D (2011) Evolutionary dynamics of feedback escape and the development of stem-cell-driven cancers. *Proc Natl Acad Sci*. pp 18983–18988.
- Werner B, Dingli D, Lenaerts T, Pacheco JM, Traulsen A (2011) Dynamics of mutant cells in hierarchical organized tissues. *PLoS Comput Biol*, (in press).
- Chomel JC, Turhan AG (2011) Chronic myeloid leukemia stem cells in the era of targeted therapies: resistance, persistence and long-term dormancy. *Oncotarget*. pp 713–727.
- Peng C, Chen Y, Li D, Li S (2010) Role of pten in leukemia stem cells. *Oncotarget* 1: 156–160.
- Vicente-Dueñas C, Abollo-Jiménez F, Ruiz-Roca L, Alonso-Escudero E, Jiménez R, et al. (2010) The age of the target cell affects b-cell leukaemia malignancy. *Aging (Albany NY)*. pp 908–913.
- Lenaerts T, Castagnetti F, Traulsen A, Pacheco JM, Rosti G, et al. (2011) Explaining the in vitro and in vivo differences in leukemia therapy. *Cell Cycle* 10: 1540–1544.
- Jiang X, Saw KM, Eaves A, Eaves C (2007) Instability of bcr-abl gene in primary and cultured chronic myeloid leukemia stem cells. *Journal of The National Cancer Institute* 99: 680–693.
- Griswold IJ, MacPartlin M, Bumm T, Goss VL, O'Hare T, et al. (2006) Kinase domain mutants of bcr-abl exhibit altered transformation potency, kinase activity, and substrate utilization, irrespective of sensitivity to imatinib. *Molecular and Cellular Biology* 26: 6082–6093.
- Skaggs BJ, Gorre ME, Ryvkin A, Burgess MR, Xie Y, et al. (2006) Phosphorylation of the atp-binding loop directs oncogenicity of drug-resistant bcr-abl mutants. *Proc Natl Acad Sci U S A* 103: 19466–19471.
- Hanfstein B, Müller MC, Kreil S, Ernst T, Schenk T, et al. (2011) Dynamics of mutant bcr-abl-positive clones after cessation of tyrosine kinase inhibitor therapy. *Haematologica* 96: 360–366.
- Dingli D, Traulsen A, Pacheco JM (2008) Chronic myeloid leukemia: origin, development, response to therapy, and relapse. *Clinical Leukemia* 2: 133–139.
- Andersson DI (2006) The biological cost of mutational antibiotic resistance: any practical conclusions? *Current Opinion in Microbiology* 9: 461–465.
- Andersson DI, Hughes H (2010) Antibiotic resistance and its cost: is it possible to reverse resistance? *Nature Reviews Microbiology* 8: 260–271.